Measurement of the Ratio of Branching Fractions $\mathcal{B}(D^0 \to K^+\pi^-)/\mathcal{B}(D^0 \to K^-\pi^+)$ using the CDF II Detector

A. Abulencia,[23] D. Acosta,[17] J. Adelman,[13] T. Affolder,[10] T. Akimoto,[55] M.G. Albrow,[16] D. Ambrose,[16] S. Amerio,[43] D. Amidei,[34] A. Anastassov,[52] K. Anikeev,[16] A. Annovi,[18] J. Antos,[1] M. Aoki,[55] G. Apollinari,[16] J.-F. Arguin,[33] T. Arisawa,[57] A. Artikov,[14] W. Ashmanskas,[16] A. Attal,[8] F. Azfar,[42] P. Azzi-Bacchetta,[43] P. Azzurri,[46] N. Bacchetta,[43] H. Bachacou,[28] W. Badgett,[16] A. Barbaro-Galtieri,[28] V.E. Barnes,[48] B.A. Barnett,[24] S. Baroiant,[7] V. Bartsch,[30] G. Bauer,[32] F. Bedeschi,[46] S. Behari,[24] S. Belforte,[54] G. Bellettini,[46] J. Bellinger,[59] A. Belloni,[32] E. Ben Haim,[44] D. Benjamin,[15] A. Beretvas,[16] J. Beringer,[28] T. Berry,[29] A. Bhatti,[50] M. Binkley,[16] D. Bisello,[43] R. E. Blair,[2] C. Blocker,[6] B. Blumenfeld,[24] A. Bocci,[15] A. Bodek,[49] V. Boisvert,[49] G. Bolla,[48] A. Bolshov,[32] D. Bortoletto,[48] J. Boudreau,[47] A. Boveia,[10] B. Brau,[10] C. Bromberg,[35] E. Brubaker,[13] J. Budagov,[14] H.S. Budd,[49] S. Budd,[23] K. Burkett,[16] G. Busetto,[43] P. Bussey,[20] K. L. Byrum,[2] S. Cabrera,[15] M. Campanelli,[19] M. Campbell,[34] F. Canelli,[8] A. Canepa,[48] D. Carlsmith,[59] R. Carosi,[46] S. Carron,[15] M. Casarsa,[54] A. Castro,[5] P. Catastini,[46] D. Cauz,[54] M. Cavalli-Sforza,[3] A. Cerri,[28] L. Cerrito,[42] S.H. Chang,[27] J. Chapman,[34] Y.C. Chen,[1] M. Chertok,[7] G. Chiarelli,[46] G. Chlachidze,[14] F. Chlebana,[16] I. Cho,[27] K. Cho,[27] D. Chokheli,[14] J.P. Chou,[21] P.H. Chu,[23] S.H. Chuang,[59] K. Chung,[12] W.H. Chung,[59] Y.S. Chung,[49] M. Ciljak,[46] C.I. Ciobanu,[23] M.A. Ciocci,[46] A. Clark,[19] D. Clark,[6] M. Coca,[15] G. Compostella,[43] M.E. Convery,[50] J. Conway,[7] B. Cooper,[30] K. Copic,[34] M. Cordelli,[18] G. Cortiana,[43] F. Cresciolo,[46] A. Cruz,[17] C. Cuenca Almenar,[7] J. Cuevas,[11] R. Culbertson,[16] D. Cyr,[59] S. DaRonco,[43] S. D'Auria,[20] M. D'Onofrio,[3] D. Dagenhart,[6] P. de Barbaro,[49] S. De Cecco,[51] A. Deisher,[28] G. De Lentdecker,[49] M. Dell'Orso,[46] F. Delli Paoli,[43] S. Demers,[49] L. Demortier,[50] J. Deng,[15] M. Deninno,[5] D. De Pedis,[51] P.F. Derwent,[16] C. Dionisi,[51] J.R. Dittmann,[4] P. DiTuro,[52] C. Dörr,[25] S. Donati,[46] M. Donega,[19] P. Dong,[8] J. Donini,[43] T. Dorigo,[43] S. Dube,[52] K. Ebina,[57] J. Efron,[39] J. Ehlers,[19] R. Erbacher,[7] D. Errede,[23] S. Errede,[23] R. Eusebi,[16] H.C. Fang,[28] S. Farrington,[29] I. Fedorko,[46] W.T. Fedorko,[13] R.G. Feild,[60] M. Feindt,[25] J.P. Fernandez,[31] R. Field,[17] G. Flanagan,[48] L.R. Flores-Castillo,[47] A. Foland,[21] S. Forrester,[7] G.W. Foster,[16] M. Franklin,[21] J.C. Freeman,[28] I. Furic,[13] M. Gallinaro,[50] J. Galyardt,[12] J.E. Garcia,[46] M. Garcia Sciveres,[28] A.F. Garfinkel,[48] C. Gay,[60] H. Gerberich,[23] D. Gerdes,[34] S. Giagu,[51] P. Giannetti,[46] A. Gibson,[28] K. Gibson,[12] C. Ginsburg,[16] N. Giokaris,[14] K. Giolo,[48] M. Giordani,[54] P. Giromini,[18] M. Giunta,[46] G. Giurgiu,[12] V. Glagolev,[14] D. Glenzinski,[16] M. Gold,[37] N. Goldschmidt,[34] J. Goldstein,[42] G. Gomez,[11] G. Gomez-Ceballos,[11] M. Goncharov,[53] O. González,[31] I. Gorelov,[37] A.T. Goshaw,[15] Y. Gotra,[47] K. Goulianos,[50] A. Gresele,[43] M. Griffiths,[29] S. Grinstein,[21] C. Grosso-Pilcher,[13] R.C. Group,[17] U. Grundler,[23] J. Guimaraes da Costa,[21] Z. Gunay-Unalan,[35] C. Haber,[28] S.R. Hahn,[16] K. Hahn,[45] E. Halkiadakis,[52] A. Hamilton,[33] B.-Y. Han,[49] J.Y. Han,[49] R. Handler,[59] F. Happacher,[18] K. Hara,[55] M. Hare,[56] S. Harper,[42] R.F. Harr,[58] R.M. Harris,[16] K. Hatakeyama,[50] J. Hauser,[8] C. Hays,[15] A. Heijboer,[45] B. Heinemann,[29] J. Heinrich,[45] M. Herndon,[59] D. Hidas,[15] C.S. Hill,[10] D. Hirschbuehl,[25] A. Hocker,[16] A. Holloway,[21] S. Hou,[1] M. Houlden,[29] S.-C. Hsu,[9] B.T. Huffman,[42] R.E. Hughes,[39] J. Huston,[35] J. Incandela,[10] G. Introzzi,[46] M. Iori,[51] Y. Ishizawa,[55] A. Ivanov,[7] B. Iyutin,[32] E. James,[16] D. Jang,[52] B. Jayatilaka,[34] D. Jeans,[51] H. Jensen,[16] E.J. Jeon,[27] S. Jindariani,[17] M. Jones,[48] K.K. Joo,[27] S.Y. Jun,[12] T.R. Junk,[23] T. Kamon,[53] J. Kang,[34] P.E. Karchin,[58] Y. Kato,[41] Y. Kemp,[25] R. Kephart,[16] U. Kerzel,[25] V. Khotilovich,[53] B. Kilminster,[39] D.H. Kim,[27] H.S. Kim,[27] J.E. Kim,[27] M.J. Kim,[12] S.B. Kim,[27] S.H. Kim,[55] Y.K. Kim,[13] L. Kirsch,[6] S. Klimenko,[17] M. Klute,[32] B. Knuteson,[32] B.R. Ko,[15] H. Kobayashi,[55] K. Kondo,[57] D.J. Kong,[27] J. Konigsberg,[17] A. Korytov,[17] A.V. Kotwal,[15] A. Kovalev,[45] A. Kraan,[45] J. Kraus,[23] I. Kravchenko,[32] M. Kreps,[25] J. Kroll,[45] N. Krumnack,[4] M. Kruse,[15] V. Krutelyov,[53] S. E. Kuhlmann,[2] Y. Kusakabe,[57] S. Kwang,[13] A.T. Laasanen,[48] S. Lai,[33] S. Lami,[46] S. Lammel,[16] M. Lancaster,[30] R.L. Lander,[7] K. Lannon,[39] A. Lath,[52] G. Latino,[46] I. Lazzizzera,[43] T. LeCompte,[2] J. Lee,[49] J. Lee,[27] Y.J. Lee,[27] S.W. Lee,[53] R. Lefèvre,[3] N. Leonardo,[32] S. Leone,[46] S. Levy,[13] J.D. Lewis,[16] C. Lin,[60] C.S. Lin,[16] M. Lindgren,[16] E. Lipeles,[9] A. Lister,[19] D.O. Litvintsev,[16] T. Liu,[16] N.S. Lockyer,[45] A. Loginov,[36] M. Loreti,[43] P. Loverre,[51] R.-S. Lu,[1] D. Lucchesi,[43] P. Lujan,[28] P. Lukens,[16] G. Lungu,[17] L. Lyons,[42] J. Lys,[28] R. Lysak,[1] E. Lytken,[48] P. Mack,[25] D. MacQueen,[33] R. Madrak,[16] K. Maeshima,[16] T. Maki,[22] P. Maksimovic,[24] S. Malde,[42] G. Manca,[29] F. Margaroli,[5] R. Marginean,[16] C. Marino,[23] A. Martin,[60] V. Martin,[38] M. Martínez,[3] T. Maruyama,[55] H. Matsunaga,[55] M.E. Mattson,[58] R. Mazini,[33] P. Mazzanti,[5] K.S. McFarland,[49] P. McIntyre,[53] R. McNulty,[29] A. Mehta,[29] S. Menzemer,[11] A. Menzione,[46] P. Merkel,[48] C. Mesropian,[50] A. Messina,[51] M. von der Mey,[8] T. Miao,[16] N. Miladinovic,[6] J. Miles,[32] R. Miller,[35] J.S. Miller,[34] C. Mills,[10] M. Milnik,[25] R. Miquel,[28] A. Mitra,[1] G. Mitselmakher,[17] A. Miyamoto,[26] N. Moggi,[5] B. Mohr,[8] R. Moore,[16] M. Morello,[46] P. Movilla Fernandez,[28] J. Mülmenstädt,[28] A. Mukherjee,[16] Th. Muller,[25] R. Mumford,[24] P. Murat,[16] J. Nachtman,[16] J. Naganoma,[57] S. Nahn,[32] I. Nakano,[40] A. Napier,[56] D. Naumov,[37] V. Necula,[17] C. Neu,[45]

M.S. Neubauer,[9] J. Nielsen,[28] T. Nigmanov,[47] L. Nodulman,[2] O. Norniella,[3] E. Nurse,[30] T. Ogawa,[57] S.H. Oh,[15] Y.D. Oh,[27] T. Okusawa,[41] R. Oldeman,[29] R. Orava,[22] K. Osterberg,[22] C. Pagliarone,[46] E. Palencia,[11] R. Paoletti,[46] V. Papadimitriou,[16] A.A. Paramonov,[13] B. Parks,[39] S. Pashapour,[33] J. Patrick,[16] G. Pauletta,[54] M. Paulini,[12] C. Paus,[32] D.E. Pellett,[7] A. Penzo,[54] T.J. Phillips,[15] G. Piacentino,[46] J. Piedra,[44] L. Pinera,[17] K. Pitts,[23] C. Plager,[8] L. Pondrom,[59] X. Portell,[3] O. Poukhov,[14] N. Pounder,[42] F. Prakoshyn,[14] A. Pronko,[16] J. Proudfoot,[2] F. Ptohos,[18] G. Punzi,[46] J. Pursley,[24] J. Rademacker,[42] A. Rahaman,[47] A. Rakitin,[32] S. Rappoccio,[21] F. Ratnikov,[52] B. Reisert,[16] V. Rekovic,[37] N. van Remortel,[22] P. Renton,[42] M. Rescigno,[51] S. Richter,[25] F. Rimondi,[5] L. Ristori,[46] W.J. Robertson,[15] A. Robson,[20] T. Rodrigo,[11] E. Rogers,[23] S. Rolli,[56] R. Roser,[16] M. Rossi,[54] R. Rossin,[17] C. Rott,[48] A. Ruiz,[11] J. Russ,[12] V. Rusu,[13] H. Saarikko,[22] S. Sabik,[33] A. Safonov,[53] W.K. Sakumoto,[49] G. Salamanna,[51] O. Saltó,[3] D. Saltzberg,[8] C. Sanchez,[3] L. Santi,[54] S. Sarkar,[51] L. Sartori,[46] K. Sato,[55] P. Savard,[33] A. Savoy-Navarro,[44] T. Scheidle,[25] P. Schlabach,[16] E.E. Schmidt,[16] M.P. Schmidt,[60] M. Schmitt,[38] T. Schwarz,[34] L. Scodellaro,[11] A.L. Scott,[10] A. Scribano,[46] F. Scuri,[46] A. Sedov,[48] S. Seidel,[37] Y. Seiya,[41] A. Semenov,[14] L. Sexton-Kennedy,[16] I. Sfiligoi,[18] M.D. Shapiro,[28] T. Shears,[29] P.F. Shepard,[47] D. Sherman,[21] M. Shimojima,[55] M. Shochet,[13] Y. Shon,[59] I. Shreyber,[36] A. Sidoti,[44] P. Sinervo,[33] A. Sisakyan,[14] J. Sjolin,[42] A. Skiba,[25] A.J. Slaughter,[16] K. Sliwa,[56] J.R. Smith,[7] F.D. Snider,[16] R. Snihur,[33] M. Soderberg,[34] A. Soha,[7] S. Somalwar,[52] V. Sorin,[35] J. Spalding,[16] M. Spezziga,[16] F. Spinella,[46] T. Spreitzer,[33] P. Squillacioti,[46] M. Stanitzki,[60] A. Staveris-Polykalas,[46] R. St. Denis,[20] B. Stelzer,[8] O. Stelzer-Chilton,[42] D. Stentz,[38] J. Strologas,[37] D. Stuart,[10] J.S. Suh,[27] A. Sukhanov,[17] K. Sumorok,[32] H. Sun,[56] T. Suzuki,[55] A. Taffard,[23] R. Takashima,[40] Y. Takeuchi,[55] K. Takikawa,[55] M. Tanaka,[2] R. Tanaka,[40] N. Tanimoto,[40] M. Tecchio,[34] P.K. Teng,[1] K. Terashi,[50] S. Tether,[32] J. Thom,[16] A.S. Thompson,[20] E. Thomson,[45] P. Tipton,[49] V. Tiwari,[12] S. Tkaczyk,[16] D. Toback,[53] S. Tokar,[14] K. Tollefson,[35] T. Tomura,[55] D. Tonelli,[46] M. Tönnesmann,[35] S. Torre,[18] D. Torretta,[16] S. Tourneur,[44] W. Trischuk,[33] R. Tsuchiya,[57] S. Tsuno,[40] N. Turini,[46] F. Ukegawa,[55] T. Unverhau,[20] S. Uozumi,[55] D. Usynin,[45] A. Vaiciulis,[49] S. Vallecorsa,[19] A. Varganov,[34] E. Vataga,[37] G. Velev,[16] G. Veramendi,[23] V. Veszpremi,[48] R. Vidal,[16] I. Vila,[11] R. Vilar,[11] T. Vine,[30] I. Vollrath,[33] I. Volobouev,[28] G. Volpi,[46] F. Würthwein,[9] P. Wagner,[53] R. G. Wagner,[2] R.L. Wagner,[16] W. Wagner,[25] R. Wallny,[8] T. Walter,[25] Z. Wan,[52] S.M. Wang,[1] A. Warburton,[33] S. Waschke,[20] D. Waters,[30] W.C. Wester III,[16] B. Whitehouse,[56] D. Whiteson,[45] A.B. Wicklund,[2] E. Wicklund,[16] G. Williams,[33] H.H. Williams,[45] P. Wilson,[16] B.L. Winer,[39] P. Wittich,[16] S. Wolbers,[16] C. Wolfe,[13] T. Wright,[34] X. Wu,[19] S.M. Wynne,[29] A. Yagil,[16] K. Yamamoto,[41] J. Yamaoka,[52] T. Yamashita,[40] C. Yang,[60] U.K. Yang,[13] Y.C. Yang,[27] W.M. Yao,[28] G.P. Yeh,[16] J. Yoh,[16] K. Yorita,[13] T. Yoshida,[41] G.B. Yu,[49] I. Yu,[27] S.S. Yu,[16] J.C. Yun,[16] L. Zanello,[51] A. Zanetti,[54] I. Zaw,[21] F. Zetti,[46] X. Zhang,[23] J. Zhou,[52] and S. Zucchelli[5]

(CDF Collaboration)

[1] *Institute of Physics, Academia Sinica, Taipei, Taiwan 11529, Republic of China*
[2] *Argonne National Laboratory, Argonne, Illinois 60439*
[3] *Institut de Fisica d'Altes Energies, Universitat Autonoma de Barcelona, E-08193, Bellaterra (Barcelona), Spain*
[4] *Baylor University, Waco, Texas 76798*
[5] *Istituto Nazionale di Fisica Nucleare, University of Bologna, I-40127 Bologna, Italy*
[6] *Brandeis University, Waltham, Massachusetts 02254*
[7] *University of California, Davis, Davis, California 95616*
[8] *University of California, Los Angeles, Los Angeles, California 90024*
[9] *University of California, San Diego, La Jolla, California 92093*
[10] *University of California, Santa Barbara, Santa Barbara, California 93106*
[11] *Instituto de Fisica de Cantabria, CSIC-University of Cantabria, 39005 Santander, Spain*
[12] *Carnegie Mellon University, Pittsburgh, PA 15213*
[13] *Enrico Fermi Institute, University of Chicago, Chicago, Illinois 60637*
[14] *Joint Institute for Nuclear Research, RU-141980 Dubna, Russia*
[15] *Duke University, Durham, North Carolina 27708*
[16] *Fermi National Accelerator Laboratory, Batavia, Illinois 60510*
[17] *University of Florida, Gainesville, Florida 32611*
[18] *Laboratori Nazionali di Frascati, Istituto Nazionale di Fisica Nucleare, I-00044 Frascati, Italy*
[19] *University of Geneva, CH-1211 Geneva 4, Switzerland*
[20] *Glasgow University, Glasgow G12 8QQ, United Kingdom*
[21] *Harvard University, Cambridge, Massachusetts 02138*
[22] *Division of High Energy Physics, Department of Physics, University of Helsinki and Helsinki Institute of Physics, FIN-00014, Helsinki, Finland*
[23] *University of Illinois, Urbana, Illinois 61801*
[24] *The Johns Hopkins University, Baltimore, Maryland 21218*
[25] *Institut für Experimentelle Kernphysik, Universität Karlsruhe, 76128 Karlsruhe, Germany*

[26] High Energy Accelerator Research Organization (KEK), Tsukuba, Ibaraki 305, Japan
[27] Center for High Energy Physics: Kyungpook National University, Taegu 702-701; Seoul National University, Seoul 151-742; and SungKyunKwan University, Suwon 440-746; Korea
[28] Ernest Orlando Lawrence Berkeley National Laboratory, Berkeley, California 94720
[29] University of Liverpool, Liverpool L69 7ZE, United Kingdom
[30] University College London, London WC1E 6BT, United Kingdom
[31] Centro de Investigaciones Energeticas Medioambientales y Tecnologicas, E-28040 Madrid, Spain
[32] Massachusetts Institute of Technology, Cambridge, Massachusetts 02139
[33] Institute of Particle Physics: McGill University, Montréal, Canada H3A 2T8; and University of Toronto, Toronto, Canada M5S 1A7
[34] University of Michigan, Ann Arbor, Michigan 48109
[35] Michigan State University, East Lansing, Michigan 48824
[36] Institution for Theoretical and Experimental Physics, ITEP, Moscow 117259, Russia
[37] University of New Mexico, Albuquerque, New Mexico 87131
[38] Northwestern University, Evanston, Illinois 60208
[39] The Ohio State University, Columbus, Ohio 43210
[40] Okayama University, Okayama 700-8530, Japan
[41] Osaka City University, Osaka 588, Japan
[42] University of Oxford, Oxford OX1 3RH, United Kingdom
[43] University of Padova, Istituto Nazionale di Fisica Nucleare, Sezione di Padova-Trento, I-35131 Padova, Italy
[44] LPNHE-Universite Pierre et Marie Curie-Paris 6, UMR7585, Paris F-75005 France; IN2P3-CNRS
[45] University of Pennsylvania, Philadelphia, Pennsylvania 19104
[46] Istituto Nazionale di Fisica Nucleare Pisa, Universities of Pisa, Siena and Scuola Normale Superiore, I-56127 Pisa, Italy
[47] University of Pittsburgh, Pittsburgh, Pennsylvania 15260
[48] Purdue University, West Lafayette, Indiana 47907
[49] University of Rochester, Rochester, New York 14627
[50] The Rockefeller University, New York, New York 10021
[51] Istituto Nazionale di Fisica Nucleare, Sezione di Roma 1, University of Rome "La Sapienza," I-00185 Roma, Italy
[52] Rutgers University, Piscataway, New Jersey 08855
[53] Texas A&M University, College Station, Texas 77843
[54] Istituto Nazionale di Fisica Nucleare, University of Trieste/ Udine, Italy
[55] University of Tsukuba, Tsukuba, Ibaraki 305, Japan
[56] Tufts University, Medford, Massachusetts 02155
[57] Waseda University, Tokyo 169, Japan
[58] Wayne State University, Detroit, Michigan 48201
[59] University of Wisconsin, Madison, Wisconsin 53706
[60] Yale University, New Haven, Connecticut 06520

(Dated: May 8, 2006)

We present a measurement of $R_{\mathcal{B}}$, the ratio of the branching fraction for the rare decay $D^0 \to K^+\pi^-$ to that for the Cabibbo-favored decay $D^0 \to K^-\pi^+$. Charge conjugate decays are implicitly included. A signal of 2005 ± 104 events for the decay $D^0 \to K^+\pi^-$ is obtained using the CDF II detector at the Fermilab Tevatron collider. The data set corresponds to an integrated luminosity of 0.35 fb^{-1} produced in $\bar{p}p$ collisions at $\sqrt{s} = 1.96$ TeV. Assuming no mixing, we find $R_{\mathcal{B}} = [4.05 \pm 0.21(\text{stat}) \pm 0.11(\text{syst})] \times 10^{-3}$. This measurement is consistent with the world average, and comparable in accuracy with the best measurements from other experiments.

PACS numbers: 13.25.Ft, 14.40.Lb

The D^0 can decay to $K^+\pi^-$ either through a doubly Cabibbo-suppressed (DCS) tree process or by oscillation (mixing) to a $\bar{D}^0$ followed by a Cabibbo-favored (CF) tree process. The charge-conjugate decays, such as $\bar{D}^0 \to K^-\pi^+$, are implied throughout this paper. The time-dependent decay rate $r(t)$ for $D^0 \to K^+\pi^-$ can be written in a compact form [1] taking into account the experimentally established facts that the rate for mixing is at least as small as that for the DCS decay, and that the effect of CP violation is small. In this formalism, and assuming CP conservation,

$$r(t) \propto e^{-\Gamma t}\left[R_D + \sqrt{R_D}y'(\Gamma t) + \frac{x'^2 + y'^2}{4}(\Gamma t)^2\right]. \quad (1)$$

The parameter R_D is the squared modulus of the ratio of DCS to CF amplitudes. The parameters x' and y' are defined in terms of the parameters $x = \Delta m/\Gamma$ and $y = \Delta\Gamma/2\Gamma$, where Δm is the difference in mass between the two mass eigenstates, $\Delta\Gamma$ is the difference in decay width between the two mass eigenstates, and Γ is the

average decay width. The definitions are

$$x' = x\cos\delta + y\sin\delta, \text{ and } y' = -x\sin\delta + y\cos\delta, \quad (2)$$

where δ is the strong phase difference between the DCS and CF amplitudes. The mixing rate is small if $x' \ll 1$ and $y' \ll 1$. The ratio of branching fractions,

$$R_{\mathcal{B}} = \mathcal{B}(D^0 \to K^+\pi^-)/\mathcal{B}(D^0 \to K^-\pi^+) \quad (3)$$

is given by the ratio of the time-integrals of the corresponding decay rates,

$$R_{\mathcal{B}} = R_D + \sqrt{R_D}y' + \frac{x'^2 + y'^2}{2}. \quad (4)$$

Thus, if x' and y' are negligible, the experimentally measurable quantity $R_{\mathcal{B}}$ can be interpreted as the theoretical parameter R_D.

In the limit of flavor SU(3) symmetry, $R_D = \tan^4\theta_C$ [2, 3] where θ_C is the Cabibbo angle, which is measured from kaon decays. The world average values [1, 4], $R_D = (3.62 \pm 0.29) \times 10^{-3}$ and $\tan^4\theta_C = (2.88 \pm 0.27) \times 10^{-3}$, are equal within their uncertainties, consistent with flavor SU(3) symmetry. However, symmetry violation of magnitude less than the current measurement accuracy is possible [5] if there are differences in the weak decay form factors $F_0^{D\pi}$ and F_0^{DK}, or due to strong interaction resonant intermediate states following the charm quark decay.

There is no experimental evidence either for CP violation in D^0 decays or for D^0-$\bar{D}^0$ mixing; all measurements are consistent with $x' = y' = 0$. An upper limit on the contribution to $R_{\mathcal{B}}$ from mixing can be derived from measured upper limits for $x', y' \sim 3 \times 10^{-2}$ [1] and the world average measurement of R_D. A simple estimate, by substituting these values into Eq. (4), gives a contribution to $R_{\mathcal{B}}$ less than 2.7×10^{-3}, a limit which is comparable to the value of R_D.

In the standard model, theoretical predictions due to short-distance weak processes are $x', y' \sim 6 \times 10^{-7}$ [6]. However, strong interaction effects could result in larger values, of order $\sin^2\theta_C$ (=0.048) times an unknown factor which describes the size of flavor SU(3) symmetry violation. Thus, accurate measurement of R_D and θ_C can establish the size of the symmetry violation factor and make possible the prediction of the standard model contribution to mixing. If the standard model contribution is small, then D^0-$\bar{D}^0$ mixing measurements will be sensitive to new physics. Theories involving weak-scale supersymmetry or new strong dynamics at the TeV scale can accommodate large values of x' and y', up to the experimental limits [7], leaving open the possibility for indirect observation of new physics.

Until now, the most precise measurements of R_D were from the B factories. The BABAR collaboration [8] reported $R_D = [3.59 \pm 0.20(\text{stat}) \pm 0.27(\text{syst})] \times 10^{-3}$ with a DCS signal of 430 events, and the Belle collaboration [9] reported $R_D = [3.81 \pm 0.17(\text{stat})\ ^{+0.08}_{-0.16}(\text{syst})] \times 10^{-3}$ with a DCS signal of 845 events. In this paper, using a DCS signal of 2005 events and assuming no mixing, we report a measurement of R_D with comparable precision to those of BABAR and Belle. As in those experiments, we reconstruct the decay chain $D^{*+} \to \pi^+ D^0$, $D^0 \to K^+\pi^-$, where the charge of the π^+ from D^{*+} decay distinguishes the D^0 from its anti-particle, $\bar{D}^0$.

Our measurement uses data collected by the CDF II detector at the Fermilab Tevatron collider, from October 2002 to August 2004. The data corresponds to an integrated luminosity of 0.35 fb^{-1} produced in $\bar{p}p$ collisions at $\sqrt{s} = 1.96$ TeV. CDF II is a multi-purpose detector with a magnetic spectrometer surrounded by a calorimeter and a muon detector. The CDF II components pertinent to this analysis are described briefly below. A more detailed description is found in [10] and references therein. A cylindrical silicon microstrip vertex detector (SVX II) [11] and a cylindrical drift chamber (COT) [12], immersed in a 1.4 T axial magnetic field, allow reconstruction of tracks (trajectories of charged particles) in the pseudo-rapidity range $|\eta| \leq 1.3$, where $\eta = \tanh^{-1}(\cos\theta)$ and θ is the angle measured from the beamline. The ionization signals from the COT provide a measurement of the specific energy loss for a charged particle, which is used for particle identification.

Events were selected in real time using a three-level trigger system with requirements developed for a broad class of heavy flavor decays. At level 1, tracks are reconstructed in the COT in the plane transverse to the beamline by a hardware processor (XFT) [13]. Two oppositely charged tracks are required, each with transverse momentum greater than 2 GeV/c. In addition, the scalar sum of the two transverse momenta must be greater than 5.5 GeV/c. The opening angle $\Delta\phi$ between the two tracks in the transverse plane must be less than 135°. At level 2, the silicon vertex tracker (SVT) [14] attaches SVX II hits to each of the two XFT tracks to increase the measurement accuracy. The transverse impact parameter d_0 is defined as the distance of closest approach, in the transverse plane, of a track to the beamline. Each of the two tracks is required to satisfy 120 μm $\leq d_0 \leq$ 1.0 mm. The opening angle cut is tightened (compared to level 1) to $2° \leq \Delta\phi \leq 90°$. The track pair forms a long-lived particle candidate which is required to have a decay length $L_{xy} > 200$ μm, where L_{xy} is the transverse distance from the beam line to the candidate's vertex, projected along the total transverse momentum of the candidate. At level 3, a conventional computer processor confirms the selection with a full event reconstruction.

The analysis method for determining the ratio of branching fractions requires reconstruction of the decay chains $D^{*+} \to \pi^+ D^0$, $D^0 \to K^-\pi^+$ (CF), and $D^{*+} \to \pi^+ D^0$, $D^0 \to K^+\pi^-$ (DCS). The D^0 candidate reconstruction starts with a pair of oppositely charged tracks that satisfy the trigger requirements. The tracks are considered with both $K^-\pi^+$ and π^-K^+ interpretations. A third track, which is required to have $p_T \geq 0.3$ GeV/c, is used to form a D^* candidate when combined as a pion with the D^0 candidate. The charge of this "tag-

ging pion" determines whether the D^0 candidate decay is CF or DCS.

To reduce systematic uncertainty, the same set of cuts is employed for both the CF and DCS decay modes. The offline analysis cuts were chosen to maximize the significance of the DCS signal determined from a study of the CF signal and the DCS background. The optimization was performed without using DCS candidates and before the candidates were revealed. The DCS signal was estimated by scaling the CF signal by the world average for R_D. The DCS background was estimated from candidates in a control region of D^* invariant mass, outside a region containing the signal. In the optimization study, the same algorithms for data analysis were followed as for the DCS signal determination.

We apply two cuts to reduce the background to the DCS signal from CF decays where the D^0 decay tracks are mis-identified. Mis-identification occurs when the kaon and pion assignments are mistakenly interchanged. This background is characterized by a $K\pi$ mass distribution with width about ten times that of the signal peak. A DCS candidate that is consistent with being a CF decay, with $K^-\pi^+$ invariant mass within $\pm$ 20 MeV/c^2 of the D^0 mass, is excluded from the DCS signal. This cut rejects 97.5% of mis-identified decays, while retaining 78% of the signal. Since the analysis procedure is the same for DCS and CF decays, a CF candidate that is consistent with being a DCS decay is excluded from the CF signal.

A cut based on particle identification from specific ionization in the COT also helps to reject mis-identified decays, but with a smaller improvement to DCS signal significance than from the cut based on invariant mass. A variable Z is defined as the ratio of logarithms of measured to predicted charge deposition for a single track. The prediction is based on the ionization expected for a particle with the measured momentum and a specific hypothesis for mass. For a pair of particles, we define

$$S_{K\pi} = \left(\frac{Z_K}{\sigma_K}\right)^2 + \left(\frac{Z_\pi}{\sigma_\pi}\right)^2 \qquad (5)$$

where the subscripts K and π indicate the particle hypotheses for the first and second track of the pair, and σ_K, σ_π are the corresponding Gaussian resolutions on Z. The particle identification for the pair is chosen by the smaller of $S_{K\pi}$ and $S_{\pi K}$. This selection is correct 80.2% of the time, as measured using the CF signal that survives the invariant mass cut.

We apply four cuts to reduce combinatoric background from prompt particle production or from improper combinations of tracks in events containing heavy flavor particles. These cuts retain most of the signal, with a small improvement in the signal significance. Since the D^0 has a long enough mean lifetime to have an observable decay length, the decay vertex should be displaced, on average, from the production point. We require the transverse decay length significance $L_{xy}/\sigma_{xy} > 5$, where L_{xy} was defined earlier and σ_{xy} is the uncertainty on

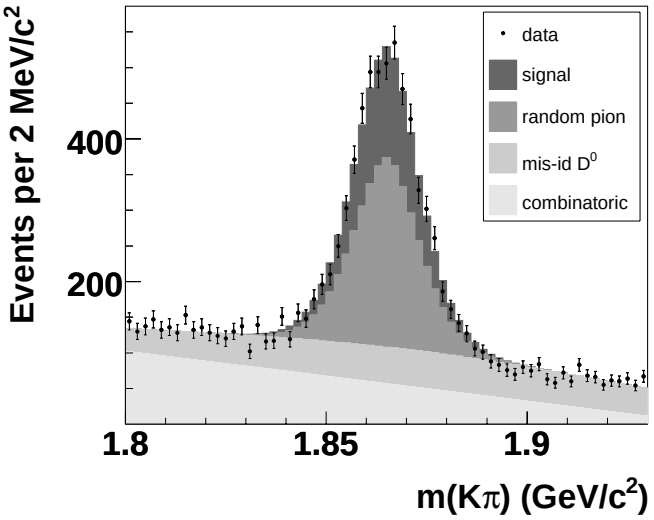

FIG. 1: $K\pi$ invariant mass distribution for candidates reconstructed as $D^0 \to K^+\pi^-$ (DCS), requiring 5 MeV/c^2 < Δm < 7 MeV/c^2. The shaded regions are projections from the overall fit onto this distribution. This mass plot illustrates the relative contributions from the DCS signal and the three types of background, as described in the text.

L_{xy}. The D^* has a short enough mean lifetime so that it should appear to decay at its production point. The tagging pion and the D^0 candidate must be consistent with coming from a common point based on a χ^2 measure in the transverse plane. For the D^* vertex, we also require $|L_{xy}/\sigma_{xy}| < 15$. Furthermore, the tagging pion track must have an impact parameter $d_0 < 800$ μm.

The $K\pi$ mass distribution for CF decays has been reported in a recent CDF II publication on singly Cabibbo-suppressed decays [15]. The $K\pi$ mass distribution for DCS candidates is illustrated by the histogram in Fig. 1 for candidates satisfying 5 MeV/c^2 < Δm < 7 MeV/c^2, where $\Delta m = m(K^+\pi^-\pi^+) - m(K^+\pi^-) - m(\pi^+)$. Four categories of $K\pi\pi$ combinations contribute to the distribution. The first category (signal) is DCS signal from D^*, with the correct $D^0 \to K^+\pi^-$ interpretation. The second category (random pion) is background from CF D^0 decays, where a randomly selected particle, usually from the primary interaction, is used as the tagging pion to form the D^* candidate. The third category (mis-id D^0) is background from D^* decays where the K and π assignments from the CF D^0 decay are mistakenly interchanged. The last category is combinatoric background, where one or both tracks do not belong to a $D \to K\pi$ decay.

To determine the signal and background, candidates are divided into 60 slices of Δm, each slice of width 0.5 MeV/c^2. (The distribution in Fig. 1 is for a 2 MeV/c^2 wide slice for purpose of illustration.) For each slice, the $K\pi$ mass distribution is fit using a binned likelihood method with a predetermined D^0 signal shape and a lin-

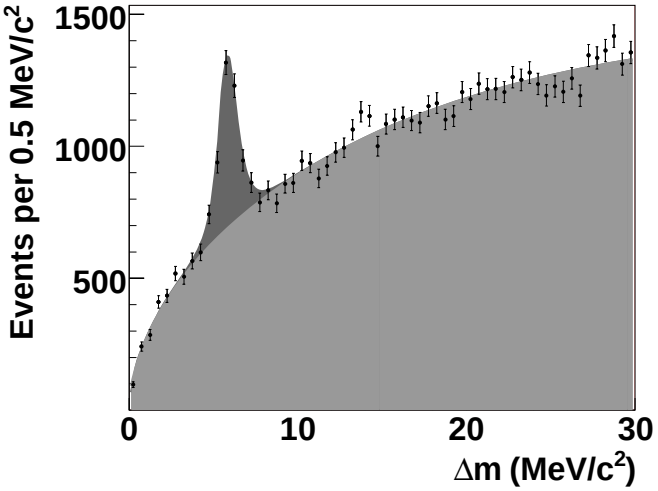

FIG. 2: The number of $D^0 \to K^+\pi^-$ (DCS) decays as a function of Δm. The data points and statistical uncertainty bars are taken from the $K\pi$ slice fits. The shaded regions are determined from a least-squares fit and show the contributions from signal (dark gray) and random tagging pion background (light gray) as explained in the text.

ear function for the background. The D^0 signal shape is determined from a fit to the CF $K\pi$ distribution, which has a negligible background compared to the signal. The fit range (1.80 - 1.93) GeV/c^2 excludes background from $D^0 \to K^+K^-$ and $D^0 \to \pi^+\pi^-$ decays that are misreconstructed as $K^+\pi^-$. The amplitude of the combined signal and random pion term and the combinatoric background parameters are allowed to float independently for each slice. The amplitude and shape of the mis-id D^0 contribution is determined from the CF signal, by interchanging the pion and kaon assignments.

To determine the amount of DCS signal and random pion background, the D^0 signal yields for the slices are plotted as a function of Δm, as shown in Fig. 2. This distribution is fit using a least-squares method with a signal shape predetermined from the CF Δm distribution and a background function of the form $A(\Delta m)^B e^{-C(\Delta m)}$. The amplitudes of the signal and background terms and the background shape parameters B and C are determined from the fit. The fit results are 2005 ± 104 DCS signal and 495172 ± 907 CF signal; their ratio gives $R_{\mathcal{B}} = (4.05 \pm 0.21) \times 10^{-3}$.

Most of the detector properties that affect the DCS and CF signals are common and hence do not affect the ratio. Thus, there are no systematic uncertainties due to geometric acceptance, particle identification, and trigger efficiency. While the number of background events is similar for the DCS and CF candidates, the size of the DCS signal is much smaller. Thus, systematic uncertainty in the DCS background which affects the DCS signal estimate also affects the ratio. There are three such significant sources of systematic uncertainty, as summarized in Table I.

To estimate the uncertainty due to the assumed combinatoric background shape in the DCS $K\pi$ slice fits, we compared $R_{\mathcal{B}}$ results for two shapes. The nominal shape is linear and gives a good fit. We also tried a quadratic form and assigned the change in $R_{\mathcal{B}}$ as a systematic uncertainty. To estimate the uncertainty due to the assumed Δm background shape, we compared $R_{\mathcal{B}}$ results for two shapes. The nominal shape is given by the function described earlier and gives a good fit. We also tried a function with an additional parameter and assigned the change in $R_{\mathcal{B}}$ as a systematic uncertainty. In fitting the DCS $K\pi$ slice fits, the amplitude of the mis-id D^0 background is fixed from the CF signal. A simulation of the fitting procedure is used to propagate the statistical uncertainty on the background amplitude to a systematic uncertainty on $R_{\mathcal{B}}$.

We considered other sources of systematic uncertainty that we found to be negligible. These include effects due to small differences in detection efficiencies for K^+ versus K^- and π^+ versus π^-, which are reported in [15]. We tried alternative fits to the DCS $K\pi$ distributions by extending the upper limit of the mass range from 1.80 to 2.00 GeV/c^2. This study required adding an explicit term for background from $D^0 \to \pi^+\pi^-$ decays.

In conclusion, we find $R_{\mathcal{B}} = [4.05 \pm 0.21(\text{stat}) \pm 0.11(\text{syst})] \times 10^{-3}$. The difference between this value and the world average value for $\tan^4\theta_C$ is $(1.17 \pm 0.34) \times 10^{-3}$, a 3.4 σ deviation from zero. If not a statistical fluctuation, this difference could be due to violation of flavor SU(3) symmetry causing $R_D \neq \tan^4\theta_C$, or could be a result of mixing. While we cannot rule out the possibility of mixing from our result alone, our result is consistent with the scenario of modest symmetry violation and negligible mixing. As shown in Fig. 3, our measured value of $R_{\mathcal{B}}$ is in fact consistent with the world average and the most accurate individual measurements of R_D obtained from BABAR [8] and Belle [9]. Using the technique we have established to extract the $D^0 \to K^+\pi^-$ signal, we can perform a time-dependent analysis using a larger data sample than reported here, to separately measure R_D and the mixing parameters x' and y'.

We thank the Fermilab staff and the technical staffs of the participating institutions for their vital contributions. This work was supported by the U.S. Department of Energy and National Science Foundation; the Italian Istituto Nazionale di Fisica Nucleare; the Ministry of Education, Culture, Sports, Science and Technology of

TABLE I: Dominant systematic uncertainties for $R_{\mathcal{B}}$. The sources lead to uncertainties in the DCS signal estimate.

Source	Uncertainty ($\times 10^{-3}$)
$K\pi$ combinatoric background shape	0.09
Δm random pion background shape	0.06
$K\pi$ mis-ID D^0 background amplitude	0.01

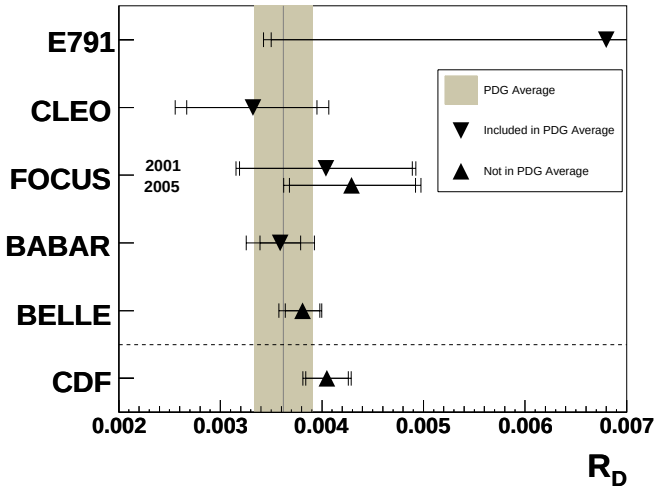

FIG. 3: Comparison of this measurement of R_D with other recent results. All the experimental fits assume no mixing or CP violation. The inner set of bars indicate statistical uncertainty; the outer set indicates the quadratic sum of statistical and systematic uncertainties. The shaded region spans the PDG average and uncertainty [1]. That average includes measurements from E791 [16], CLEO [17], FOCUS(2001) [18], and BABAR [8]. The Belle [9], FOCUS(2005) [19] and current CDF measurements are not included in the PDG average.

Japan; the Natural Sciences and Engineering Research Council of Canada; the National Science Council of the Republic of China; the Swiss National Science Foundation; the A.P. Sloan Foundation; the Bundesministerium für Bildung und Forschung, Germany; the Korean Science and Engineering Foundation and the Korean Research Foundation; the Particle Physics and Astronomy Research Council and the Royal Society, UK; the Russian Foundation for Basic Research; the Comisión Interministerial de Ciencia y Tecnología, Spain; in part by the European Community's Human Potential Programme under contract HPRN-CT-2002-00292; and the Academy of Finland.

[1] S. Eidelman *et al.* (Particle Data Group), Phys. Lett. B **592**, 1 (2004), review by D. Asner on $D^0 - \bar{D}^0$ mixing.
[2] R. L. Kingsley, S. B. Trieman, F. Wilczek and A. Zee, Phys. Rev. D **11**, 1919 (1975).
[3] M. B. Voloshin, V. I. Zakharov and L. B. Okun, Pis'ma Zh. Eksp. Teor. Fiz. **21**, 403 (1975) [JETP Lett. **21**, 183 (1975)].
[4] *Ibid.* [1], review by E. Blucher and W.J. Marciano on V_{ud}, V_{us}, the Cabibbo angle, and CKM Unitarity.
[5] M. Gronau and J. L. Rosner, Phys. Lett. B **500**, 247 (2001).
[6] E. Golowich and A. A. Petrov, Phys. Lett. B **625**, 53 (2005).
[7] G. Burdman and I. Shipsey, Annu. Rev. Nucl. Sci. **53**, 431 (2003). See section 2.3.
[8] B. Aubert *et al.* (BABAR Collaboration), Phys. Rev. Lett. **91**, 171801 (2003).
[9] K. Abe *et al.* (Belle Collaboration), Phys. Rev. Lett. **94**, 071801 (2005).
[10] D. Acosta *et al.* (CDF Collaboration), Phys. Rev. D **71**, 032001 (2005).
[11] A. Sill *et al.*, Nucl. Instrum. Methods **A447**, 1 (2000).
[12] T. Affolder *et al.*, Nucl. Instrum. Methods **A526**, 249 (2004).
[13] E. J. Thomson *et al.*, IEEE Trans. Nucl. Sci. **49**, 1063 (2002).
[14] W. Ashmanskas *et al.*, Nucl. Instrum. Methods **A518**, 532 (2004).
[15] D. Acosta *et al.* (CDF Collaboration), Phys. Rev. Lett. **94**, 122001 (2005).
[16] E. M. Aitala *et al.* (E791 Collaboration), Phys. Rev. D **57**, 13 (1998).
[17] R. Godang *et al.* (CLEO Collaboration), Phys. Rev. Lett. **84**, 5038 (2000).
[18] J. M. Link *et al.* (FOCUS Collaboration), Phys. Rev. Lett. **86**, 2955 (2000).
[19] J. M. Link *et al.* (FOCUS Collaboration), Phys. Lett. B **618**, 23 (2005).